J Mater Sci (2007) 42:5875–5879
DOI 10.1007/s10853-006-1001-z

Dielectric behavior of Cu–GeO_2 cermet thin films

Irine Banu Lucy

Received: 7 July 2004 / Accepted: 30 August 2005 / Published online: 24 May 2007

Abstract Capacitance and dielectric loss measurements were carried out using an Al/Cu–GeO_2/Al sandwich structure for 0 to 10 vol% Cu films, 120–400 nm thick, deposited at 0.4–1.5 nm/s in the frequency and temperature range 1–10^6 Hz and 90–573 K, respectively. The variation of capacitance and dielectric loss with frequency and temperature follows the Goswami and Goswami model. Capacitance decreases slowly with increasing thickness and also varies with the change in deposition rate of the cermet film.

Introduction

Cermet films have been studied for more than half a century and the many new properties revealed have led to a continuing interest in such films [1–6]. The properties of cermet films can be adjusted by varying the composition, deposition rate, thickness, deposition temperature, etc. and consequently, this material has found varied applications in the microelectronics industry. These include resistors, capacitors and inductors, electro-mechanical sensors, heating elements, memory and switching devices, thermoelectric conversion elements and thin film magnetic heads [7, 8]. Since a large number of properties of these films undergo rapid changes with temperature, the material can be used in a variety of thermal devices such as thermal detectors, thermometers, thermocouples [9] etc. In this paper the capacitance and loss tangent of Cu–GeO_2 cermet films have been investigated using Metal–Insulator–Metal (MIM) sandwich structure.

I. B. Lucy (✉)
Department of Physics, University of Rajshahi,
Rajshahi 6205, Bangladesh
e-mail: irine@librabd.net

Experimental procedure

Cu–GeO_2 thin cermet films used in this study were prepared by vacuum co-evaporation of high purity Cu and GeO_2 in a Speedivac 19A/122 coating unit onto clean Corning 7059 glass substrate at a pressure of 1 mPa. Molybdenum boats were used for the co-evaporation of Cu and GeO_2. The capacitance and loss tangent measurements were carried out using a Hewlett–Packard Impedance analyser (Model 4192) in the frequency range 1 kHz to 1 MHz in the temperature range 90–600 K. The measuring range of capacitance was 0.1 pF to 0.1 F and of loss angle 1×10^{-4} to 19.99. All have a basic accuracy of ±0.1%. The ac signal applied across the electrodes was 0.5 V (rms) with zero dc bias.

Figure 1 shows the schematic diagram of experimental set up for capacitance and loss tangent measurements. Three identical sandwich structures were formed on the substrate using suitable masks. The bottom and top electrodes were connected through highly polished small Cu blocks connected on L-shaped Cu stripes. The Cu stripes were mounted on top of ceramic and PTFE rectangular blocks to insulate the electrodes from the massive Cu holder. A rectangular ceramic heater was placed inside the Cu block holder to raise the temperature of the sample and liquid nitrogen was used via the sample holder stainless steel tank to lower the sample temperature.

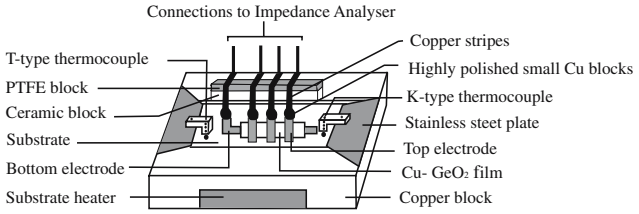

Fig. 1 Schematic diagram of experimental set up

T and K type thermocouples were used to measure the temperature of the sample in the range of 90–300 K and 300–600 K, respectively. The zero offset adjustments were made to avoid any error due to cable lengths. Measurements were carried out on Al/Cu–GeO_2/Al sandwich structures with 0–10 vol% Cu films in the temperature range 90–573 K. The Cu–GeO_2 cermet films were deposited on a substrate maintained at a temperature of 600 K.

Results and discussions

Variation of capacitance with frequency, composition and temperature

The capacitance of 0–10 vol% Cu–GeO_2 films, 200 nm thick, deposited at a rate of 0.8 nm/s was measured as a function of frequency between 10^3 Hz and 10^6 Hz. The dependence of capacitance on frequency at 300 K is shown in Fig. 2. It can be seen that the capacitance decreases with frequency up to 200 kHz and thereafter becomes independent of frequency. The variation is less pronounced in the lower metal volume fraction (<2vol% Cu) samples. Figure 3 is a capacitance versus temperature graph at 10 kHz. It can be seen that capacitance is strongly temperature-dependent at higher temperatures and that all the curves tend to saturate to constant values below 160 K. Similar results have been obtained for Al–Dy_2O_3–Al [10], Al–CdTe–Al [11], Al–SiO/SnO_2–Al [12], Au–CuPc–Au [13] and Au–CoPc–Au [14] films.

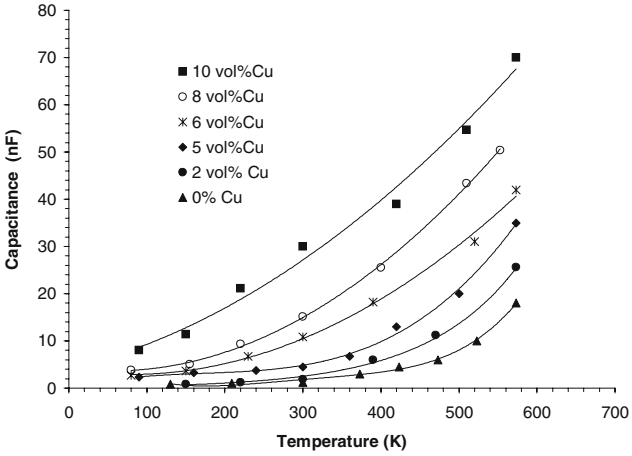

Fig. 3 Variation of capacitance with temperature at 10 kHz of various compositions of Cu–GeO_2 films

Figure 4 shows how capacitance depends on frequency at selected temperatures in a 5 vol% Cu sample. As can be seen, the capacitance of the device increases with temperature. The change in capacitance is more pronounced at higher temperatures (>360 K) and frequencies below 200 kHz. Below 160 K the capacitance is almost independent of frequency in the sample. Rahman [15] with electron-beam evaporated planar structures of Al/Cu–GeO_2/Al also found that capacitance increases with increase in substrate temperature during measurement and shows very little dependence on frequency above 100 kHz and below

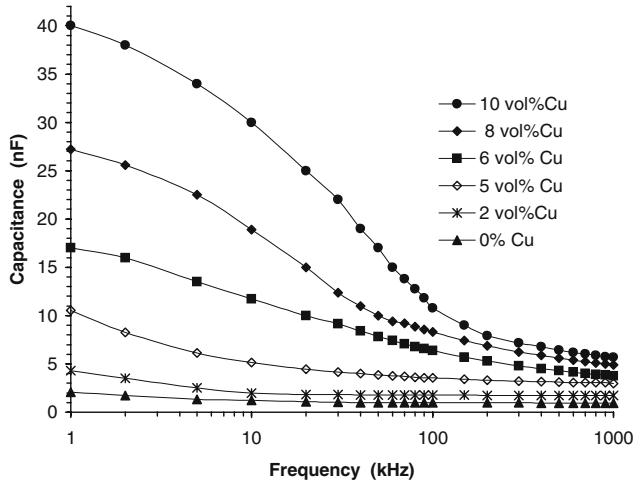

Fig. 2 Variation of capacitance versus frequency of various compositions of Cu–GeO_2 films at 300 K

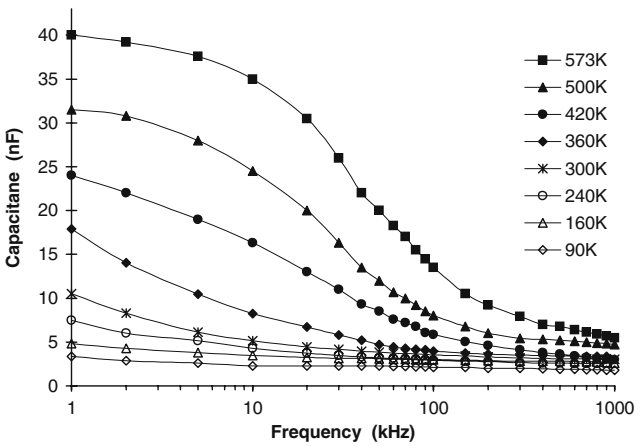

Fig. 4 Variation of capacitance versus frequency of a 5 vol% Cu film at selected temperatures

250 K. He also found that capacitance tended to a constant value at around 150 K. Hence there is very good agreement between Cu–GeO_2 films prepared by co-evaporation and electron-beam evaporation. The major difference is that the capacitance in this investigation was ~10^{-9} F while Rahman's [15] value was ~10^{-13} F.

A MIM sandwich configuration is similar to a parallel plate capacitor, the capacitance of which is given by Harrop [16]

$$C = \varepsilon_0 \varepsilon_r \frac{A}{d} \quad (1)$$

where ε_o is the dielectric constant of free space (=8.85 × 10^{-12} Fm^{-1}), ε_r is the relative dielectric constant of the thin film material, A is the active area of the device (4 mm^2) and d is the thickness of the film. Since capacitance increases with increase in metallic content, ε_r is also a function of Cu content.

The increase in capacitance with increase in Cu content may possibly be explained as follows. As the metallic content of the film increases, the number of metallic islands increase and the inter-island separation decreases. This results in an increase of micro-capacitors formed by the metallic islands and a decrease in plate separation, thereby increasing the capacitance.

Variation of loss tangent with frequency, composition and temperature

The variation in tan δ with frequency at 300 K for 0 – 10 vol% Cu–GeO_2 is shown in Fig. 5; tan δ possesses a minimum value for all compositions studied. It can be seen that tan δ_{min} shifts towards higher numerical values and higher frequencies as the Cu content of the sample increases. In Fig. 6 tan δ is plotted versus frequency at selected temperatures for 5 vol% Cu. Tan δ possesses a minimum in all cases with ω_{min} shifting towards higher frequencies at higher temperatures. Figure 7 shows how ω_{min} varies with temperature for Cu–GeO_2 films of various compositions. It is obvious that not only does ω_{min} increase with increasing Cu content; it also increases gradually with increasing temperature.

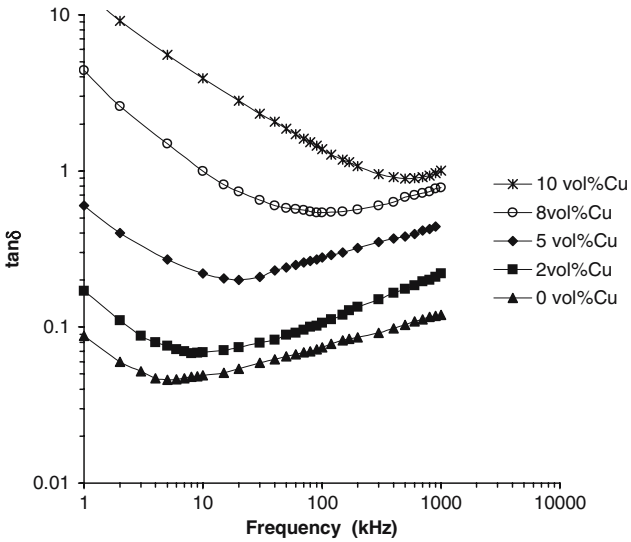

Fig. 5 Variation of tan δ versus frequency at 300 K for various compositions of Cu–GeO_2 films

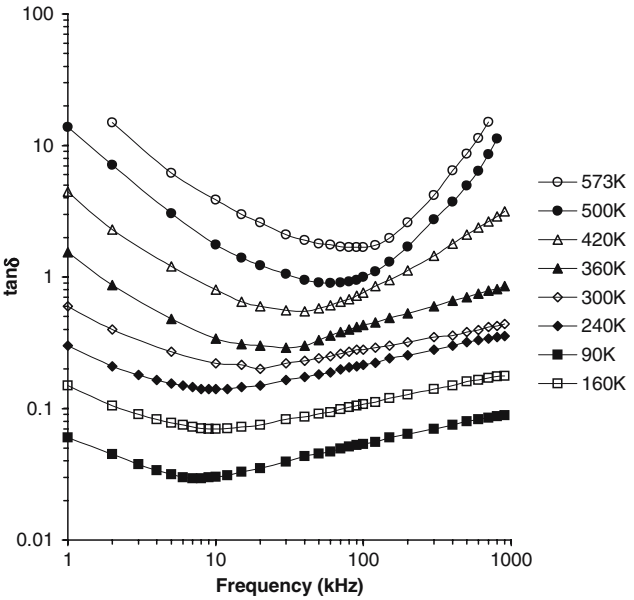

Fig. 6 Variation of tan δ versus frequency at selected temperatures of a 5 vol% Cu film

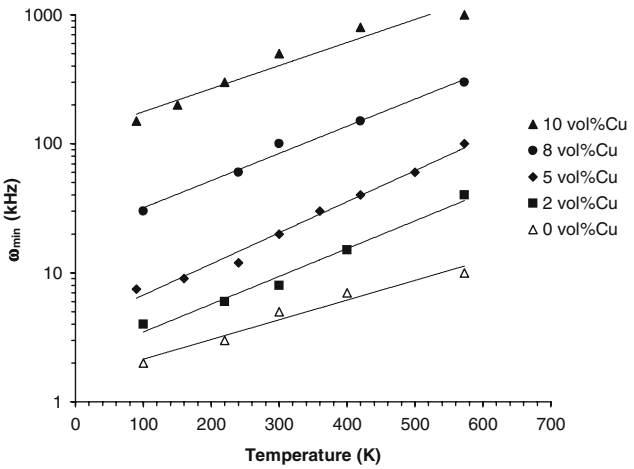

Fig. 7 Variation of loss minima with temperatures of various compositions of Cu–GeO_2 samples

The occurrence of $\tan\delta_{min}$ at a particular frequency ω_{min} and the shift in $\tan\delta_{min}$ towards higher frequencies with increase in temperature may be explained using the model of Goswami and Goswami [17]. According to this model each capacitor system is assumed to comprise: (i) an inherent capacity element C unaffected by frequency and temperature; (ii) a discrete resistance element R due to the dielectric film in parallel with C, and (iii) a series resistance r due to the leads. Figure 8a and b show the different elements and the equivalent series circuit C_s and R_s where

$$C_s = C + \frac{1}{\omega^2 R^2 C} \quad (2)$$

and

$$R_s = r + \frac{R}{1 + \omega^2 R^2 C}$$

In general $R \gg r$, with r assumed to have a constant value, whilst R will be affected by temperature due to the exponential factor in the relation

$$R = R_o \exp\frac{\Delta E}{kT}$$

Where R_o is a constant and ΔE is the activation energy. According to the Goswami model, $\tan\delta$ can be written as $\tan\delta = \frac{1}{\omega RC} + \omega rC$

When ω is small $1/\omega RC \gg \omega rC$, and

$$\tan\delta = \frac{1}{\omega R C} \quad (3)$$

When ω is large, $1/\omega RC$ is generally $\ll \omega rC$, and

$$\tan\delta = \omega r C \quad (4)$$

Equation (3) shows that $\tan\delta$ decreases with increasing frequency and Eq. (4) shows that $\tan\delta$ increases with increasing frequency. Thus $\tan\delta$ must pass through a minimum. On Eqs. (3) and (4), ω_{min} is given by

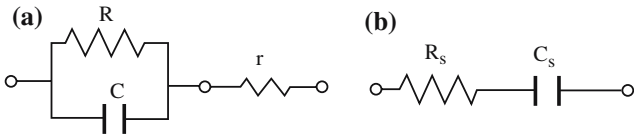

Fig. 8 Goswami and Goswami model (**a**) capacitor elements (**b**) equivalent circuit

$$\omega_{min} = \frac{1}{(r\,R\,C^2)^{1/2}}$$

Since R increases with decrease in temperature and r remains practically unchanged, ω_{min} must also decrease at lower temperatures. Thus ω_{min} is expected to shift towards lower frequencies as the temperature is lowered.

The effect of temperature on capacitance can be considered from Eq. (2). At low temperatures (high R) or high frequency, or both, $1/\omega^2 R^2 C \ll C$ giving $C_s = C$. Thus at a particular temperature and frequency, capacitance is expected to be independent of both temperature and frequency. This result is confirmed in co-evaporated Cu–GeO_2 films below 160 K and above 200 kHz. However, the theory is at variance with the discussion following Eq. (1) in which the relative permittivity ε_r is stated to be a function of capacitance; ε_r does not appear in the Goswami and Goswami [17] model.

Variation of capacitance with thickness

Figure 9 shows the variation of capacitance with inverse thickness for 5 vol% Cu samples at 300 K. Capacitance decreases slowly with increasing thickness. The variation is linear and agrees with Eq. (1).

Variation of capacitance with deposition rate

Figure 10 shows capacitance versus deposition rate graph of 10 vol% Cu films at 300 K. Capacitance increases gradually with increasing deposition rate. It can be seen that capacitance increases almost linearly

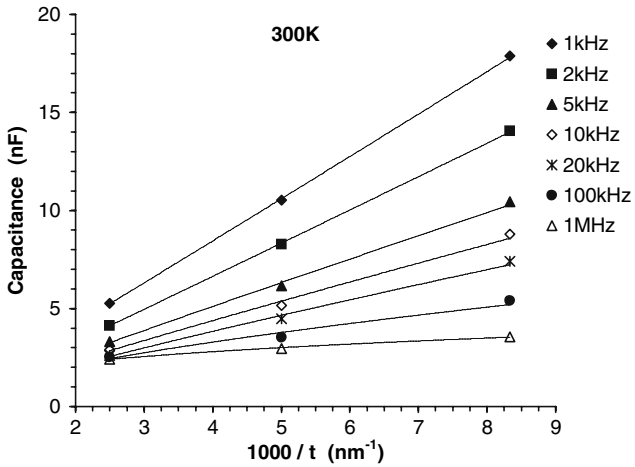

Fig. 9 Variation of capacitance with inverse thickness at selected frequencies of 5 vol% Cu samples at 300K.

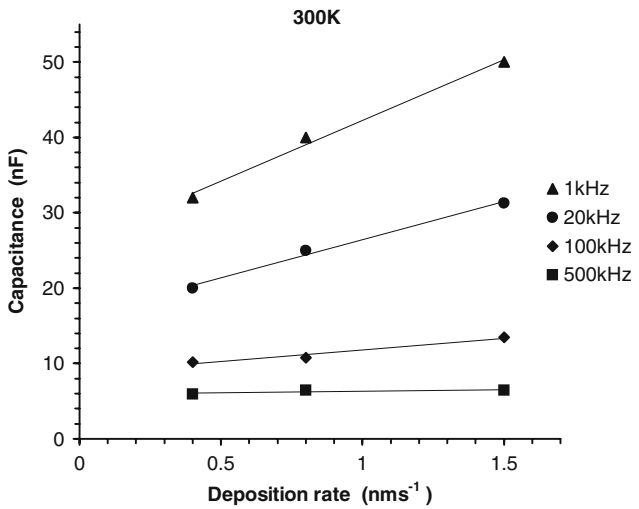

Fig. 10 Variation of capacitance versus deposition rate at selected frequencies of 10 vol% Cu samples at 300 K

with deposition rate below 100 kHz and is almost independent of deposition rate at 500 kHz.

From dc conductivity measurements [18] it is found that conductivity increases with increasing deposition rate. Following the model of Goswami and Goswami [17] using Eq. (2), C_s is expected to increase linearly with increasing conductivity and hence with deposition rate. At very high frequencies (>500 kHz) capacitance is also expected to attain a constant value independent of deposition rate or conductivity.

Summary

In Cu–GeO_2 cermet film (0–10 vol%) ac capacitance increases with increase in temperature and deposition rate of the film and decreases with the increase in frequency (10^3–10^6 Hz). Loss tangent has a minimum that shifts towards higher frequencies with increasing metal volume fraction. Loss tangent also increases with the increase in substrate temperature. All of these observations lend support to Goswami and Goswami model.

Acknowledgements I am grateful to Dr. John Beynon of Brunel University, UK for his enthusiastic guidance throughout this work and to Prof. C. A. Hogarth of the same University for many useful discussions.

References

1. Lucy IB (2004) J Mat Sci 39:3163
2. Zaidi SZA, Beynon J, Steele CB (1997) J Mat Sci 32(15):3921
3. Hosseini AA, Hogarth CA, Beynon J (1994) J Mat Sci Lett 13:1144
4. Steele CB, Beynon J, Hogarth CA, (1992) Thin Solid Films 213:76
5. Lucy IB, (1999) Ind J Pure Appl Phy 37:836
6. Rahman MH, Al Saie AM, Beynon J (2000) J Mat Sci 35(23):5899
7. Nava F, Tien T, Tu KN (1984) J Appl Phys 33(1):74
8. Ohring M, (1992) The materials science of thin films. Academic Press Inc., New York, p 508
9. Chopra KL, Das SR (1983) Thin film solar cells. Plenum Press and Publications
10. Goswami A, Verma RR (1975) Thin Solid Films 28:157
11. Dharmadhikari VS (1983) Int J Electronics 54(6):787
12. Rahman ASMS, Islam MH, Hogarth CA (1987) Int J Electronics 62(5):685
13. Gould RD, Hassan AK (1993) Thin Solid Films 223:334
14. Shihub SI, Gould RD (1995) Thin Solid Films 254:187
15. Rahman MH (1995) PhD thesis, Dept. of Physics, Brunel University, Uxbridge, Middlesex, UK
16. Harrop PJ (1972) Dielectrics Butterworth & Co Publishers Ltd., London, Uk, p 4
17. Goswami A, Goswami AP (1973) Thin Solid Films 16:185
18. Lucy IB (2000) J Mat Sci 35:4567